A novel microelectrochemical strategy for the study of corrosion inhibitors employing the scanning vibrating electrode technique and dual potentiometric/amperometric operation in scanning electrochemical microscopy

Javier Izquierdo[a], Lívia Nagy[b], Juan J. Santana[a,c], Géza Nagy[b], Ricardo M. Souto[a,d]

[a] *Department of Physical Chemistry, University of La Laguna, E-38200 La Laguna, Tenerife, Canary Islands, Spain*

[b] *Department of General and Physical Chemistry, Faculty of Sciences, University of Pécs, 7624 Pécs, Ifjúság útja 6, Hungary*

[c] *Department of Process Engineering, University of Las Palmas de Gran Canaria, E-35017 Las Palmas de Gran Canaria, Canary Islands, Spain*

[d] *Instituto de Materiales y Nanotecnologías, University of La Laguna, E-38200 La Laguna, Tenerife, Canary Islands, Spain*

Abstract

A combined scanning microelectrochemical procedure is proposed to obtain information on the action of corrosion inhibitors on metals. The method uses the scanning vibrating electrode technique (SVET) and the scanning electrochemical microscopy (SECM). Antimony tips are employed as the sensing probe in SECM, allowing this technique to be operated in both potentiometric and amperometric modes. This novel approach allows the spatial distributions of pH, concentration of redox active species, and ionic currents associated to corrosion processes to be monitored. The model system employed for such investigation was the galvanic corrosion of an iron/copper couple immersed in sodium chloride solution. The procedure is used to investigate *in situ* the effect of benzotriazole (BTAH) on the cathodic half-cell reaction on copper. A big decrease of electrochemical activity on copper occurs as result of the formation of inhibitor-containing films on the surface of the metal, which hinder the cathodic process on the copper surface to such an extent that cathodic sites may eventually develop on the less noble iron surface, in addition to the anodic sites. That is, inhibition of the cathodic reaction on copper by BTAH effectively renders this metal inactive, though electrically connected to the iron specimen, thus reducing the galvanic coupling between the two metals. That supports the idea that BTAH acts as cathodic inhibitor.

Keywords: Scanning electrochemical microscopy; scanning vibrating electrode technique; corrosion inhibition; pH distribution; antimony microelectrode.

1. **Introduction**

Corrosion processes on metal electrodes can be inhibited by organic and inorganic molecules adsorbed to the metal surface. The formation of surface films containing these molecules may either retard metal dissolution or hinder the corresponding cathodic processes, rendering the protected metal more resistant against the attack of species present in the environment. Characterization of metal-inhibitor systems is frequently based on the use of conventional electrochemical techniques, though they average the response of relatively large specimen areas and they provide little information on the mechanism of the chemical interactions and processes which have their origin in micro- and nanometric scales. The recent development of scanning microelectrochemical techniques which are operated *in situ*, thus closely matching the natural conditions occurring during aqueous corrosion, are greatly contributing to a more detailed and efficient characterization of corrosion systems in general, and of corrosion inhibition more particularly. The introduction of scanning electrochemical microscopies to corrosion studies was due to Isaacs [1-3], when the scanning vibrating electrode technique (SVET) was employed to detect pathways for ionic currents above corroding metals. The vibrating probe actually measures potential differences in the electrolytic phase in contact with the corroding metal arising from the fluxes of ionic species that participate in the electrochemical reactions occurring at the metal/solution interface. Since then, this technique has found application to investigate a wide variety of corrosion processes and to characterize the protection properties of many surface films applied on metals [4], though a major limitation of the technique is the impossibility to identify the species that cause the ionic flux. A promising route to overcome this limitation has been offered by the use of ion-selective microelectrodes as a non-vibrating probe to potentiometrically monitor the concentration distributions of charged species in the solution adjacent to the surface under investigation [5,6]. This is the operation principle of the scanning ion-selective electrode technique (SIET) [7].

The electrochemical reactivity of a metal/electrolyte interface can be imaged with the scanning electrochemical microscope (SECM) [8]. This technique is based on the reaction that occurs at a mobile ultramicroelectrode tip (UME) immersed in an electrolyte solution in close vicinity of a surface [9], which is an amperometric electrochemical operation. Both the topography and/or redox activity of the solid/liquid interface can be characterized from the faradaic current measured at the tip [9]. Despite its more recent introduction in corrosion science, this technique has already found even wider application due to its higher spatial resolution and chemical selectivity [10-12]. Yet, some specific difficulties concerning the use of SECM have been reported when metal systems bearing redox potentials more negative than oxygen electroreduction [13-15] and/or hydrogen evolution were investigated. Another limitation is the observation of interferences to the detection of some redox systems due to the presence of other electrochemically-reactive species involved in the overall corrosion process which effectively affect the chemical selectivity of the technique [16]. In the

first case, non-aqueous environments had to be employed for the investigation of the electrochemical reactivity of the metallic systems [13,14], whereas higher chemical selectivity would be required to solve the later. This is the reason to investigate the applicability of the potentiometric operation in SECM [17,18] for the study of corrosion reactions [19], though from a practical point of view, it is very difficult to control the tip-sample distance in this case. A very promising way to combine the advantages of amperometric and potentiometric operation modes in SECM has arisen from the introduction as UME tips of materials that exhibit a dual-function in different potential ranges [20,21]. This is the case with antimony, a material that changes its open circuit potential in response to the pH of the environment [17]

The issue of corrosion inhibition of metallic surfaces is becoming increasingly addressed employing scanning microelectrochemical techniques. Most of the available studies make use of SVET, whereas SECM has been employed scarcely. In the later case, only the copper-benzotriazole (BTAH) system has been investigated so far. Yet, those studies have shown the utility of SECM to monitor the kinetics of inhibitor film formation [22-25], which is derived from the progressive decrease in the conductive characteristics of the surface with the elapse of time. Furthermore, simple and fast operation procedures can be employed to inter-compare the inhibition efficiencies of Cu-BTAH films formed under different pre-treatments [25,26], as well as their resistance to the corrosive attack of aggressive environments [27]. Despite these outstanding advantages, it has not been possible to identify the half cell reaction affected by the presence of the benzotriazole-containing surface film exclusively on the basis of those experiments. Indeed, this effect remains to be controversial through the scientific literature [28-34]. Thus, there is need to design new experiments to characterize localized electrochemical activity on corroding systems by monitoring the spatial distributions of pH, redox active species, and ionic currents associated to the corrosion reactions.

In the present report, we describe SVET and SECM characterization of the pH distribution, oxygen consumption and ionic current flows related to the galvanic corrosion of an iron-zinc pair exposed to aqueous chloride solution. One of the specific goals of this work is to explore the ability of benzotriazole to inhibit the cathodic reaction during copper corrosion. To accomplish this, the copper surface has been pre-treated with benzotriazole for different times to form surface films of varying thickness, and consequently detect any variation in the distribution of anodic and cathodic sites between the two metals. Dual potentiometric and amperometric operation of the SECM has been achieved using antimony microelectrodes as tips [21].

2. Experimental

2.1. SVET instrumentation and experimental procedure

The scanning vibrating electrode instrumentation used was manufactured by Applicable Electronics Inc. (Forestdale, MA, USA) and controlled by dedicated software. The probe microelectrode consisted of Pt/Ir (80%/20%) wires insulated with paralene C® and arced at the tip to expose the metal, and they were platinized in order to produce a spherical platinum black deposit of 10-20 μm diameter. A video camera connected to an optical microscope was introduced in the system both to establish the probe to sample distance, and to follow the movement of the vibrating electrode over the sample during operation. The measurements were made with the electrode tip vibrating both normal (frequency, 200 Hz; amplitude, 37.5 μm) and parallel (frequency, 100 Hz; amplitude, 20 μm) to the sample mounted horizontally facing upwards. The mean distance between the microelectrode and the sample surface was 80 μm.

2.2. SECM instrumentation and experimental procedure

The scanning electrochemical microscope was a home-built system [35] that used a 3D positioning device driven by precision step motors with 75 nm minimal step size. A video camera was used to further assist positioning of the tip close to the surface. The distance between the tip and the substrate was established by allowing the probe to gently rest on the sample, and subsequently the probe was retracted to the chosen operation distance with the aid of the *Z*-positioning motor. In order to achieve dual potentiometric/amperometric operations with one single probe, an antimony microelectrode with a 25 μm diameter active disk surface at the tip was employed. The procedures employed both in the fabrication of the antimony microelectrode, and in the determination of its pH sensing performance are described in detail elsewhere [21]. In brief, the electrode was calibrated from the measurement of the potential response transients toward pH change of the solution, using a sequence of seven buffer solutions covering the $3 < pH \leq 11.5$ range. **Figure 1** is the calibration curve of the electrode's potential response to the pH value of the solution, which shows a good linear relationship. The slope of the line is 46.1 mV/pH unit.

SECM experiments were carried out in a three-electrode cell. The antimony tip was the working electrode, an Ag/AgCl/3M KCl reference electrode and a platinum counter electrode. Specimens were mounted horizontally facing upwards. The measurements were performed with the microelectrode at a height of 25 μm over the specimen surface.

2.3. Materials

The testing samples consisted of iron and copper wires (dia. 0.7 mm) mounted into an Epofix (Struers, Ballerup, Denmark) resin sleeve, so that only their cross sections area formed the testing metal substrate (see **Figure 2**). For the galvanic couple experiments the two electrodes embedded in the resin could be connected electrically at the back of the mount. The mounts with the samples were polished with silicon carbide paper down to 800 grit, and subsequently polished with alumina micropolish of 1 and of 0.3 μm particle size. The resulting surfaces were thoroughly rinsed with Millipore deionised water, dried with acetone and finally surrounded laterally by sellotape, thus creating a container for the test electrolyte solution.

Reagents of analytical grade and twice-distilled water were employed to prepare all the solutions. Microelectrochemical measurements and surface preparation processes were performed at ambient temperature in the naturally aerated solutions. Corrosion tests were carried out in aqueous 10 mM NaCl solution. Inhibitor solution was prepared at a 1 mM concentration by dissolving BTAH in a 0.1 M Na_2SO_4 solution. Inhibitor films were produced on the copper electrode *ex-situ* by dipping the portion of the mount containing the copper wire in the inhibitor-containing solution for three different immersion times (5, 30, and 60 min, respectively) which were selected from the characteristic behaviours of the surface films formed on copper that were observed in a previous study from our group at La Laguna [25].

3. Results and discussion

The inhibitory action of benzotriazole (BTAH) on copper has been investigated using scanning microelectrochemical techniques which provide spatially resolved information on the reactivity of surfaces, particularly in relation to the effect of this organic molecule on the cathodic half cell reaction. Ionic current fluxes, pH changes and concentration variations of chemical species can be gathered using an experimental methodology based on the scanning vibrating electrode technique (SVET) and scanning electrochemical microscopy (SECM).

The experimental system considered in order to check the validity of the proposed method was an iron-copper galvanic couple, and the inhibitor was put in contact with the copper specimen exclusively. The two metals were chosen in order that copper would be the nobler metal, thus securing this metal to be free from the development of local anodes throughout the experiments. The behaviour of the two metals without electrical connection in the test environment was also investigated as a reference system. The rationale for this case was to gain further information on the inhibitory effect of BTAH on copper, which ideally would result in the total blockage of the metal in case of a 100% inhibition efficiency, effectively leaving the iron sample as the only active metal

surface in the system. Inhibitor films were formed on the copper specimen from their immersion in 1 mM BTAH + 0.1 M Na_2SO_4 solution for different treatment times. The duration of the treatments considered in this work, namely 5, 30 and 60 min, were chosen on the basis of the trends observed in a previous work on the kinetics of inhibitor film formation for the Cu-BTAH system using the same conditioning procedure [25] as to match the main states revealed in that investigation. Another objective of this investigation was to explore the effect of pH on the corrosion of iron. Galvanic coupling of iron to copper leads to the removal of the cathodic reaction from the iron surface. This reaction is responsible for the alkalinisation of the electrolyte next to the reactive site. In this way, it will take longer for the iron specimen to be exposed to an alkaline environment, thus effectively preventing the precipitation of corrosion products on this metal, a situation usually found during the spontaneous corrosion of iron in otherwise neutral aqueous electrolytes.

3.1. Characterization of the galvanic coupling of iron and copper by SVET

The scanning vibrating electrode technique measures ionic fluxes in the electrolytic phase next to a corroding surface. In a neutral environment, the distribution of anodic sites can be revealed from the flux of cations departing from the surface as result of the dissolution reaction of the metal, whereas anions will be produced at the cathodic sites. The chemical reactions responsible for these ionic fluxes can be written as:

$$Fe \rightarrow Fe^{2+} + 2e^- \quad (1)$$

$$O_2 + 2H_2O + 4e^- \rightarrow 4OH^- \quad (2)$$

The sign of the ionic species departing from the surface in each half cell reaction can be followed from the opposite sign of the potential gradients produced in the electrolyte as a result of their transport.

Figure 3 depicts the images generated by SVET of different experimental conditions of an iron-copper galvanic couple immersed in 10 mM NaCl. The images were always taken after a fixed period of immersion in the electrolyte, namely 120 minutes, in order to directly relate any changes in the activity of the samples to the differences in the experimental conditions applied to the metals. The case of the inhibitor-free metal surfaces will be considered first, when the metals were either electrically disconnected (Figure 3A) or electrically connected to form the galvanic pair (Figure 3B). In the first case, ionic fluxes are only observed above the iron wire because of the greater tendency to corrode of this metal compared to copper in this environment. The anodic reaction is found to be greatly localized over a small portion of the iron surface, whereas the corresponding cathodic

process is distributed on the surrounding metal area almost concentrically. The magnitude of the fluxes measured for both processes is also an indication of the relative areas of anodic and cathodic sites distributed on the metal. The smaller size of the anodic site is responsible for the greater ionic flux associated to the dissolution of metal ions, whereas the release of hydroxyl ions is distributed over a wider area and smaller ion fluxes are measured at each point. The situation changes significantly in relation to the distribution of the anodic and cathodic reactions when the two metals are put in electric contact. In this case, the anodic process continues to occur on a small portion of the iron sample, whereas the cathodic process is mainly shifted to the copper sample, where it is found to distribute quite homogeneously over the totality of the metal surface. Yet some cathodic activity remains on the surrounding iron surface, as it could be expected because the two metals are at the same potential and the anodic activity occurs only in a portion of the iron surface. Another relevant feature is the observation of bigger electrochemical activity for the galvanic pair compared to the isolated metals. That is, the corrosive process on the iron specimen is facilitated by the displacement of the cathodic activity to the copper surface.

The electrochemical activity in the galvanic pair is reduced in a great extent when the copper surface is covered by a BTAH-containing film as shown in the sequence of images in Figure 3 C-E. Not only the total activity decreases in the system, but it is observed that the cathodic activity is shifted from the copper to the iron surface as the inhibitor film on copper is thicker. Eventually, for the thickest protective film, corresponding to the 60 min treatment of the copper specimen in the inhibitor-containing solution, it is found a situation closely matching that previously observed on iron when it was electrically disconnected from copper (cf. Figure 3A and 3E). Yet, a more detailed observation of Figure 3E in the region of the copper sample allows a very small cathodic activity to be detected. The inhibiting effect of BTAH on the cathodic reaction in copper has thus been revealed through this sequence of images taken by SVET.

The influence of the BTAH films deposited on copper towards the inhibition of the cathodic reaction is also deduced from the inspection of the SVET images given in Figure 4, which were recorded after 600 min immersion of the iron-copper galvanic pairs in the 10 mM NaCl test solution. Thicker BTAH films on copper help to greatly reduce the extent of galvanic corrosion on the coupled metals (cf. Figures 4 A-B), until the copper wire becomes so effectively blocked that the cathodic reaction has to occur quantitatively on the iron specimen together with the anodic sites. These more aggressive conditions were chosen for the experiments using the SECM as described in he next Section.

3.2. Characterization of the galvanic coupling of iron and copper by SECM

In order to better examine the corrosion reactions of the iron-copper galvanic pair and the origin of the inhibiting effect of BTAH on copper metal, SECM using an antimony tip was used. The antimony tip in potentiometric SECM allows pH distributions in the electrolyte next to the galvanic pair to be monitored, whereas the conventional amperometric operation could be used to follow the consumption of oxygen in the system in the course of the corrosion reaction. In the later case, the tip potential was set at -0.65 V vs. Ag/AgCl/3M KCl.

The extent and location of the different active areas on the metals during their exposure to the 10 mM NaCl test solution could be imaged by acquiring bidimensional scans over the center of both iron and copper samples of the metal which give the local distribution of pH as shown in Figure 5. When the metal specimens were exposed to the test electrolyte without electric connection (i.e. no galvanic coupling exists in the system), pH changes can be observed only in the proximity of the iron sample (see Figure 5A). That is, the onset of corrosion occurs on this metal, whereas copper stays basically unreactive in this electrolyte, which is consistent with the absence of ionic currents over this metal in the corresponding SVET measurements (cf. Figure 3A),. The two half cell reactions take place on the corroding iron, and significant alkalinisation of the electrolyte occurs in the proximity of the metal as it should be expected from equation (2). The highest pH values are observed shortly after immersion in the electrolyte, and less alkaline environments are found as time elapses. And after 190 min exposure, the pH of the solution volume next to the iron sample exhibits the typical values of the bulk electrolyte, which evidences that the corrosion process has been suppressed. It is also interesting to notice that the exact location on the iron surface at which the maximum pH values are observed in each pH distribution line moves progressively from left to right in the plots. The highest pH values are observed thus at the beginning of the experiment, with a maximum value of ca. 9 in the pH scale. All the observed results can be explained by considering that the surface becomes progressively blocked by the precipitation of iron-containing corrosion products, thus leading to the local anodes and cathodes to move when the precipitates blocked the surface. This feature was observable even with the naked eye, and it is shown in the optical micrographs given in Figure 6 which were taken for both wires just at the beginning of the experiment (image A) and after 3 hours exposure (image B). The shift of the pH distribution peaks from left to right in Figure 5A with the elapse of time is an indirect observation that the anodic dissolution reaction initially happened in a region close to the left border of the iron wire, and it progressed to the right as the anodic sites were getting blocked by the precipitation of corrosion products. This shift of the anodic activity towards the right side, produces a reduction in the area available for the cathodic reaction that becomes progressively more confined to the right side of the sample. On the other, the pH of the volume of electrolyte directly in contact with the copper wire

does not change during the duration of the experiment, and the local pH values coincide with those of the bulk electrolyte.

Conversely to the situation described in the previous paragraph, separation of the anodic and cathodic sites between the two metals occur when the two metals are galvanically coupled in the same test electrolyte as shown in Figure 5B. In this case, alkalinisation occurs exclusively above the copper wire. The dissolution of iron is enhanced as result of the galvanic coupling process, thus leading to significantly more alkaline environments in the electrolyte adjacent to the cathode. In fact, the highest pH observed over isolated iron was ca. 9 just after immersion in the electrolyte (see Figure 5A), but values in the proximity of 11 are measured over copper in electrically connected with iron (cf. Figure 5B). Furthermore, the iron dissolution process is not blocked by corrosion products this time, and it seems to progress at rather constant rate. This feature is due to the spatial separation of the anodic and cathodic half cell reactions on the two metals, which are placed at sufficient distance for the precipitation of corrosion product not to occur on the surface of the iron metal, which would eventually lead to blockage of the reactive surface, but on the resin between the two metals. In this way, the local pH above iron remains at the initial value of the bulk electrolyte during all the experiment.

The effect of benzotriazole on the iron-copper galvanic corrosion reaction was also investigated from the measurement of bidiomensional local pH line scans for samples subjected to different pre-treatment durations in a solution containing the inhibitor. Figure 5 C-E presents a selection of the lines measured at different exposures in the test solution of samples where the copper surfaces were pre-treated with BTAH for 5, 30 and 60 minutes, respectively. Major changes in both the shape and the evolution of the local pH distributions given by the line scans are evident from their comparison with the corresponding line scans measured for the untreated copper surface given in Figure 5B. Though the pH distribution values above the copper wire treated with BTAH for 5 minutes are still very similar to those measured for the untreated metal, some changes can already be observed in Figure 5C. Firstly, the electrolyte solution above iron is slightly more alkaline than in the previous case, which indicates the onset of some small cathodic activity on the iron wire. Though a defective inhibiting film on copper was formed in this case, yet it provides some blocking effect to the cathodic reaction on copper that leads to the observation of additional cathodic activity on the iron surface. Furthermore, the iron dissolution is restricted to a small area on the surface, allowing for a small peak at the left related to local acidification to be seen as result of the occurrence of the hydrolysis reaction of iron according to:

$$Fe^{2+} + n\,H_2O \rightarrow Fe(OH)_n^{2-n} + n\,H^+ \qquad (3)$$

The protective characteristics of the BTAH film formed on copper are very weak and the cathodic activity is increasingly concentrated on this metal with the elapse of time.

A more pronounced effect of BTAH on the galvanic corrosion process is observed as thicker films are produced on copper. Figure 5D shows the local pH distribution line scans measured for a sample pre-treated for 30 minutes with BTAH. In this case, the initial cathodic activity is observed to occur on the surface of both metals to almost the same extent thus resulting in two alkalinisation peaks with their maxima at ca. pH = 10. Therefore, the corrosion reaction is less vigorous than in the case of the untreated copper sample (Figure 5B), though the system is more active than for the isolated iron specimen in the same electrolyte (Figure 5). Another interesting observation is that the inhibitor film is not compact enough to withstand the aggressive electrolyte, and with the elapse of time the cathodic reaction becomes progressively concentrated on the copper wire. Increased alkalinisation of the electrolyte above the copper sample is thus observed, whereas the pH values above iron coincide with those of the bulk electrolyte for exposures in excess of 1 hour.

Analogously, the line scans measured when the copper sample was pre-treated with BTAH for 1 hour show the occurrence of both anodic and cathodic half-cell reaction on the surface of iron, and the copper surface is almost completely inactive at the beginning of the experiment. The localization of the dissolution reaction on the surface of iron leads to the observation of an acidification peak in the first line scan just above the site of the anodic reaction. The activation of the copper surface for the cathodic reaction can be observed at longer exposures, which is an indication of the little stability of the inhibitor films formed on copper simply by dipping the freshly polished metal in the solution containing the organic molecule. Indeed, the amperometric operation of the SECM for the electroreduction of oxygen shows the existence of two zones of depleted oxygen concentration in the electrolyte located above both metal wires after 3 hours exposure in the test electrolyte (see Figure 7). Though the pH line shows that the electrolyte is more acidic above the iron metal, the past cathodic activity of this metal has resulted in a volume of depleted oxygen concentration. On the other hand, the onset of the cathodic reaction on copper at a later time has resulted in the simultaneous depletion of oxygen and the alkalinisation of the electrolyte above this metal. Figure 7 is considered to provide a strong evidence of the great applicability of the combined potentiometric/amperometric operation of SECM for the in situ study of the evolution of corrosion reactions with high spatial resolution.

The distinctive activation process of the cathodic reaction on copper after immersion in the case of the metal protected by BTAH films can be observed with greater precision from the time evolution of the pH maximum values over the metal that are depicted in Figure 8. The cathodic

reaction occurs exclusively on copper in the case of the untreated sample, and pH values around 11 are observed at all times. In the case of the 5 minutes pre-treatment with BTAH, the surface film is very thin and eventually does not cover the copper surface completely, and thus only a very weak inhibiting effect against galvanic corrosion being provided as revealed by pH values around 10.5 in the electrolyte next to the surface of this metal. The formation of a rather effective inhibiting film on copper is then observed for the sample pre-treated with BTAH for 30 minutes. Yet the film is not stable enough to withstand the aggressivity of the test electrolyte for the duration of the experiment, and progressive activation of the cathodic activity on the metal is observed this time. After ca. 1 hour, the BTAH film on copper is not longer protective, and pH values similar to those measured in the previous cases are found. Finally, pH values below 9 are observed above the metal at all times in the case of the inhibitor films formed during 60 minutes. Furthermore, the progressive activation of the copper surface with the elapse of time can be followed from the plot obtained with this method, and this will be a measure of the persistence of the inhibitor film on the metal. Thus, the novel methodology presented in this work may have a great applicability to the investigation of the stability inhibitor films for corrosion protection.

The anodic reaction occurring on iron can be investigated from the minimum pH values of the electrolyte directly above the metal in a similar manner. Figure 9A shows their time evolution for the different specimens considered in our work. Local acidification of the electrolyte is observed in all the case, though different trends can also be found in this figure among the different systems. Firstly, the dissolution of iron in a galvanic pair in which copper is not protected by an inhibiting film, leads to local acidification of the electrolyte for almost an hour, and then a constant pH value is observed for the remaining of the experiment. The dissolution reaction progresses at a constant velocity that helps to maintain the pH of the electrolyte despite the opposite effect of diffusion of the ionic species to the bulk of the electrolyte. No suppression of the corrosion reaction due to the precipitation of corrosion products occur in the galvanic pair system. Acidification of the electrolyte above iron for about one hour prior to the attainment of a constant pH value also occurs when the copper sample has been pre-treated with BTAH for both 5 minutes, and the pH plateau shows a slightly more acidic value than for the untreated sample. No efficient inhibition of the corrosion process is provided by the surface film formed by BTAH on copper by dipping during 5 minutes the metal in the inhibitor containing solution. A different situation is found when copper was treated for 30 minutes with BTAH. Both the anodic and cathodic reactions occur initially on the iron surface, and the high localization of the anodic site leads to the development of a more acidic environment. It is only after ca. 1 hour that the cathodic reaction is shifted to the copper surface (cf. figures 7 and 8), and by then the electrolyte is more acidic and the system requires extra time before the rate of

acidification starts to decrease. Indeed, the inflection point towards the development of a stationary pH value for this system may be found for times longer than 100 minutes.

Finally, the curve given in Figure 9A for the system where copper was pre-treated for 60 minutes with BTAH closely resembles that of the untreated copper. This is an indication of the physical separation of the anodic and cathodic sites in the system. In the case of the untreated system, this fact was evident as the anodic reaction occurs on one metal and the cathodic on the other. But, now both the anodic and the cathodic reactions must occur on iron as result of the effective inhibitor effect of BTAH on copper. Indeed, Figure 9B shows that the occurrence of the cathodic reaction on iron for all the duration of the experiment as described by the maximum pH values measured on this metal. And the special behaviour of this system is then observed. Both local acidification and alkalinisation occur simultaneously over different regions of the iron sample, and they remain in practically the same locations for the duration of the experiment, thus effectively resulting in a permanent separation of the anodic and cathodic sites. This is consistent with the observation of local acidification on iron at the same location above iron in Figure 5E at all times, and the cathodic reaction on this metal remains on another location as long as cathodic occurs on this metal, though the onset of the cathodic reaction on copper as well.

In summary, the combined amperometric/potentiometric operations of SECM allow local pH distributions and the concentration of different species to be (quasi) simultaneously imaged for corrosion reactions. But it has been demonstrated that this novel methodology allows for additional information on the kinetics of these processes to be gained because very precise measurements of local changes can be detected, certainly at much earlier times they can be evidenced by ex situ methods or by less sensitive in situ microelectrochemical techniques that operate at longer probe-substrate distances. A distinctive finding of this work was the situation represented in Figure 7, when the cathodic reaction had already been removed from the iron to the copper surface as demonstrated by the local acidification above iron, and yet the past cathodic on the same metal could be detected from the depleted oxygen concentration in the same small volume of electrolyte. These findings may have a great potential for the investigation of real systems of greater complexity such of those occurring during the corrosion of alloys for aerospace applications in which diverse forms of localized and galvanic corrosion take place on the same portion of material.

4. Conclusions

Scanning electrochemical microscopy (SECM) operated with combined potentiometric/amperometric modes allows more information on the dynamics of corrosion processes to be gathered in the same experiment. The use of antimony microelectrodes as tips make possible to measure local distributions of pH above corroding systems, whereas amperometrically detecting the species participating in the corrosion reactions. In addition, the scanning vibrating electrode technique (SVET) was employed to assist the unambiguous localization of the cathodic and anodic half cell reactions in the corroding system.

The corrosion protection efficiency of the films formed by the inhibitor benzotriazole on copper, and their stability in an aggressive electrolyte without reservoir of the inhibitor molecule could be determined in the same experiment by using the scanning microelectrochemical techniques SECM and SVET.

The galvanic coupling of copper with iron, if the metals are sufficiently separated, produces an increase in the dissolution rate of iron since the precipitation of corrosion products does not occur on this metal. Otherwise, the surface would have been blocked by the corrosion products and the corrosion reaction would have significantly been slowed.

Benzotriazole forms surface films on copper that inhibit the cathodic half cell reaction on this metal, and may eventually lead to the both cathodes and anodes to be formed simultaneously on iron though the two metals are in electric contact during exposure to the same electrolyte.

Acknowledgements:

The authors are grateful to the Spanish Ministry of Science and Innovation (MICINN, Madrid, Acción Integrada No. HH2008-0011) and to the National Office for Research and Technology (NKTH, Budapest, research grant ES-25/2008 TeT) for the grant of a Collaborative Research Programme between Hungary and Spain. J.I., J.J.S. and R.M.S. are grateful for financial support by the MICINN and the European Regional Development Fund (Brussels, Belgium) under Project No. CTQ2009-12459. A Research Training Grant awarded to J.I. by the MICINN (*Programa de Formación de Personal Investigador*) is gratefully acknowledged.

References:

1. H.S. Isaacs, Corros. Sci. 28 (1988) 547.
2. H.S. Isaacs, J. Electrochem. Soc. 138 (1991) 722.

3. M.J. Franklin, D.C. White, H.S. Isaacs, Corros. Sci. 33 (1992) 251.
4. R.S. Lillard, in: P. Marcus, F. Mansfeld (Eds.), Analytical methods in corrosion science and engineering; CRC Press, Boca Raton, FL, 2006, p.571.
5. S.V. Lamaka, O.V. Karavai, A.C. Bastos, M.L. Zheludkevich, M.G.S. Ferreira, Electrochem. Commun. 10 (2008) 259.
6. S.V. Lamaka, M.G. Taryba, M.L. Zheludkevich, M.G.S. Ferreira, Electroanalysis 21 (2009) 2447.
7. S.V. Lamaka, R.M. Souto, M.G.S. Ferreira, in: A. Méndez-Vilas, J. Díaz (Eds.), Microscopy: Science, technology, applications and education, Vol. 3; Formatex Research Center, Badajoz (Spain), 2010, p. 2162.
8. J. Kwak, A.J. Bard, Anal. Chem. 61 (1989) 1221.
9. A.J. Bard, M.V. Mirkin (Eds.), Scanning electrochemical microscopy; Marcel Dekker, New York, 2001.
10. S.E. Pust, W. Maier, G. Wittstock, Z. Phys. Chem. 222 (2008) 1463.
11. L. Niu, Y. Yin, W. Guo, M. Lu, R. Qin, S. Chen, J. Mater. Sci. 44 (2009) 4511.
12. R.M. Souto, S.V. Lamaka, S. González, in: A. Méndez-Vilas, J. Díaz (Eds.), Microscopy: Science, technology, applications and education, Vol. 3; Formatex Research Center, Badajoz (Spain), 2010, p. 1769.
13. I. Serebrennikova, H.S. White, Electrochem. Solid-State Lett. 4 (2001) B4.
14. I. Serebrennikova, S. Lee, H.S. White, Faraday Discuss. 121 (2002) 199.
15. Y. González-García, R.M. Souto, S. Daniele, J. Phys. Chem. C, submitted.
16. R.M. Souto, J.J. Santana, L. Fernández-Mérida, S. González, Electrochim. Acta 56 (2011) in press.
17. B. Horrocks, M.V. Mirkin, D.T. Pierce, A.J. Bard, G. Nagy, K. Toth, Anal. Chem. 65 (1993) 1213.
18. G. Nagy, L. Nagy, Anal. Lett. 40 (2007) 3.
19. Á. Varga, L. Nagy, J. Izquierdo, I. Bitter, R.M. Souto, G. Nagy, Anal. Lett. 43 (2011) in press.
20. B. Czoka, Z. Mekhalif, Electrochim. Acta 54 (2009) 3225.
21. J. Izquierdo, L. Nagy, J.J. Santana, R.M. Souto, G. Nagy, Electrochem. Commun. Submitted.
22. K. Mansikkamäki, P. Ahonen, G. Fabricius, L. Murtomäki, K. Kontturi, J. Electrochem. Soc. 152 (2005) B12.
23. K. Mansikkamäki, C. Johans, K. Kontturi, J. Electrochem. Soc. 153 (2006) B311.
24. K. Mansikkamäki, C. Johans, K. Kontturi, J. Electrochem. Soc. 153 (2006) B22.
25. J. Izquierdo, J.J. Santana, S. González, R.M. Souto, Electrochim. Acta 55 (2010) 8791.
26. M. Pähler, J.J. Santana, W. Schuhmann, R.M. Souto, Chem. Eur. J. 17 (2011) 905.
27. J.J. Santana, M. Pähler, R.M. Souto, W. Schuhmann, Langmuir, submitted.
28. M. Sugimasa, L.-J. Wan, J. Inukai, K. Itaya, J. Electrochem. Soc. 149 (2002) E367.
29. D.-Q. Zhang, L.-X. Gao, G.-D. Zhou, Corros. Sci. 46 (2004) 3031.

30. A.M. Abdullah, F.M. Al-Kharafi, B.G. Ateya, Scripta Mater. 54 (2006) 1673.
31. D.M. Bastidas, Surf. Interf. Anal. 38 (2006) 1146.
32. K.L. Stewart, J. Zhang, S. Li, P.W. Carter, A.A. Gewirth, J. Electrochem. Soc. 154 (2007) D57.
33. M.M. Antonijević, S.M. Milić, M.B. Petrović, Corros. Sci. 51 (2009) 1228.
34. N.K. Allam, A.A. Nazeer, E.A. Ashour, J. Appl. Electrochem. 39 (2009) 961.
35. B. Kovács, B. Csóka, G. Nagy, I. Kapui, R.E. Gyurcsányi, K. Tóth, Electroanalysis 11 (1999) 349.

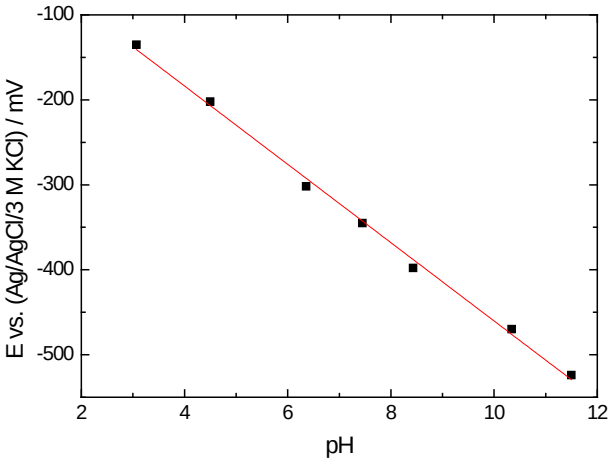

Figure 1
Calibration curve for the antimony microelectrode tip for pH measurement.

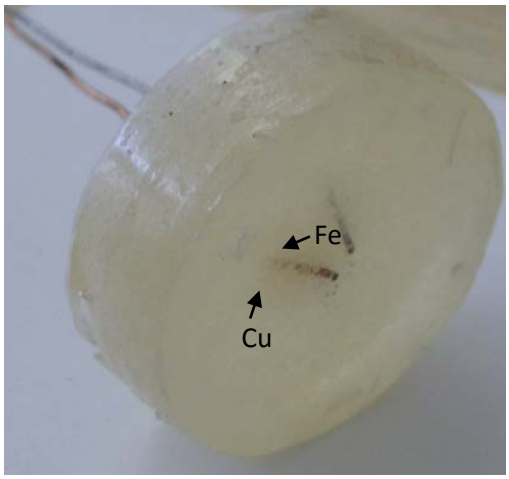

Figure 2

Photograph showing the lateral view of the iron-copper galvanic pair embedded in an insulating sleeve. The electrical connection was made at the rear of the mould.

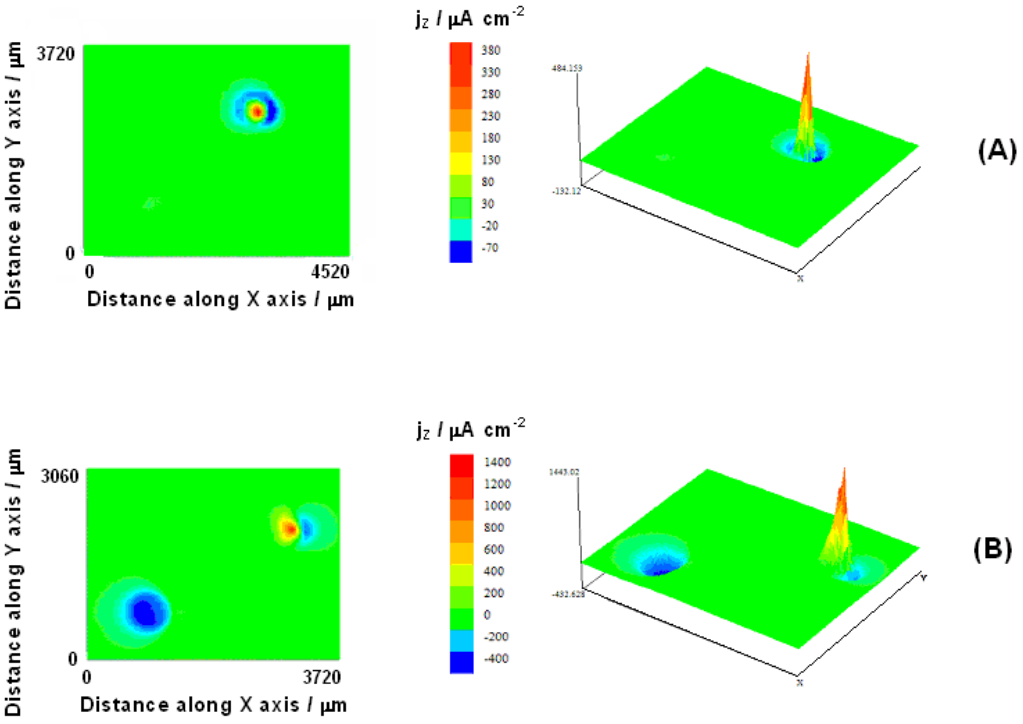

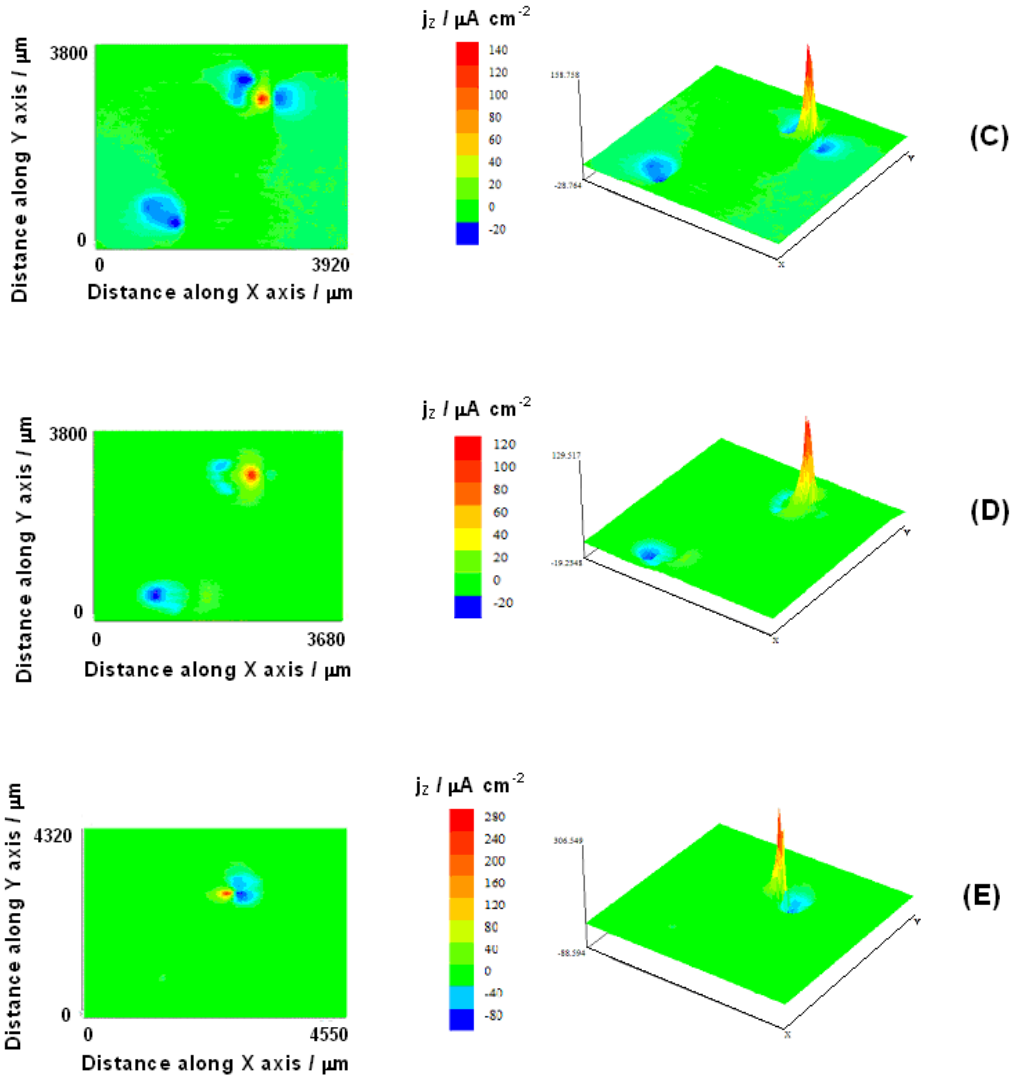

Figure 3

Images generated by SVET of different experimental conditions of an iron-copper sample. The samples were immersed in 10 mM NaCl. BTAH-containing surface films were prepared on the copper by dipping only the part of the mount with the wire in 1 mM BTAH + 0.1 M Na_2SO_4 solution for selected times as given below. Electric condition of the metal wires: (A) electrically insulated, i.e. there is no galvanic coupling; and (B-E) electrically connected to form a galvanic pair. Surface condition of the copper sample: (A-B) The metal has not been pretreated with BTAH; duration of pretreatment with BTAH: (C) 5 min, (D) 30 min, and (E) 60 min. The mounts with the metal wires were maintained in the test solution for 120 min before the SVET image was recorded. Tip-substrate distance: 80 µm.

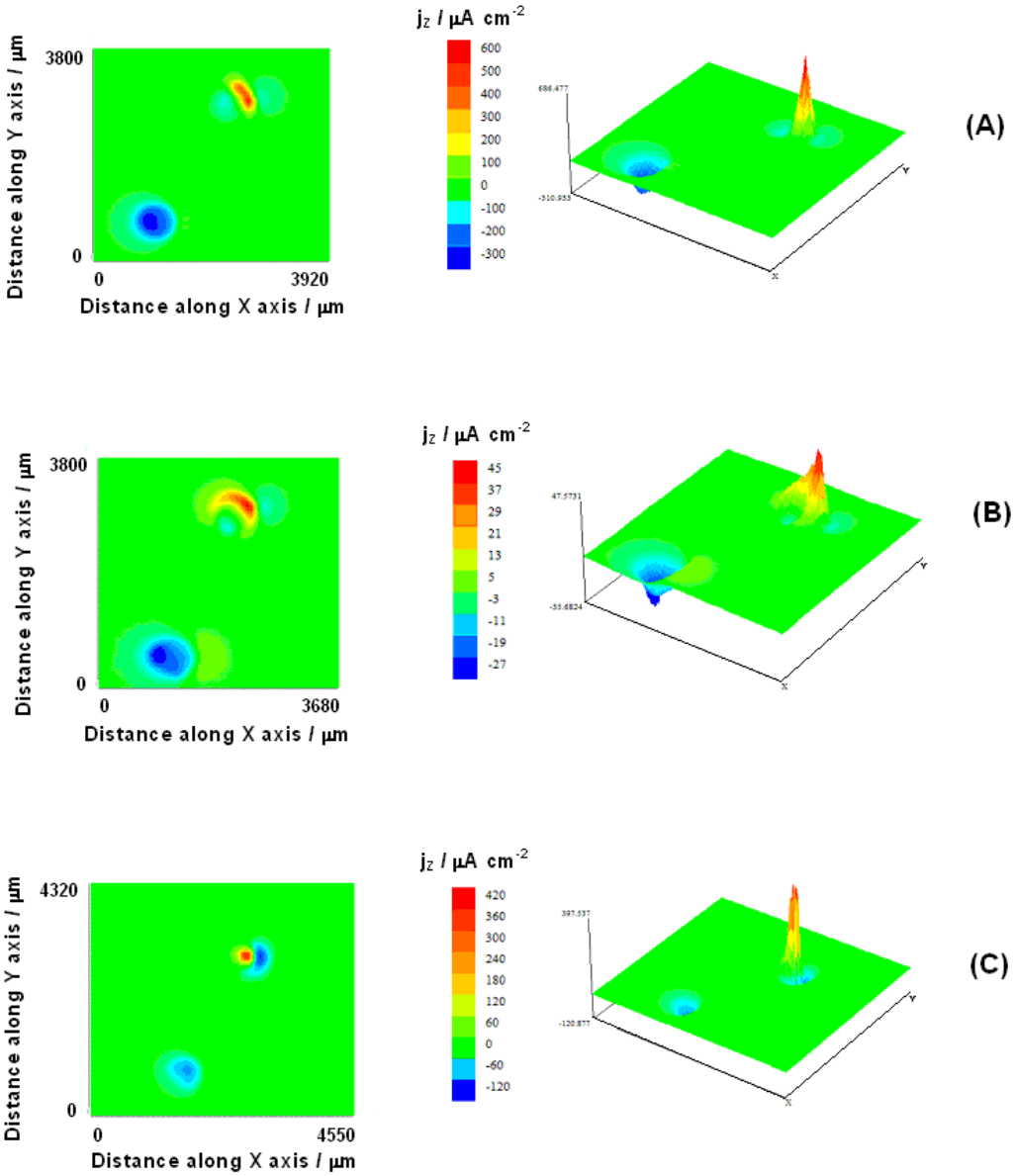

Figure 4

Images generated by SVET of iron-copper galvanic pairs immersed in 10 mM NaCl for 600 min before the SVET image was recorded. The copper specimen was pretreated in 1 mM BTAH + 0.1 M Na_2SO_4 solution for: (A) 5 min, (B) 30 min, and (C) 60 min. Tip-substrate distance: 80 µm.

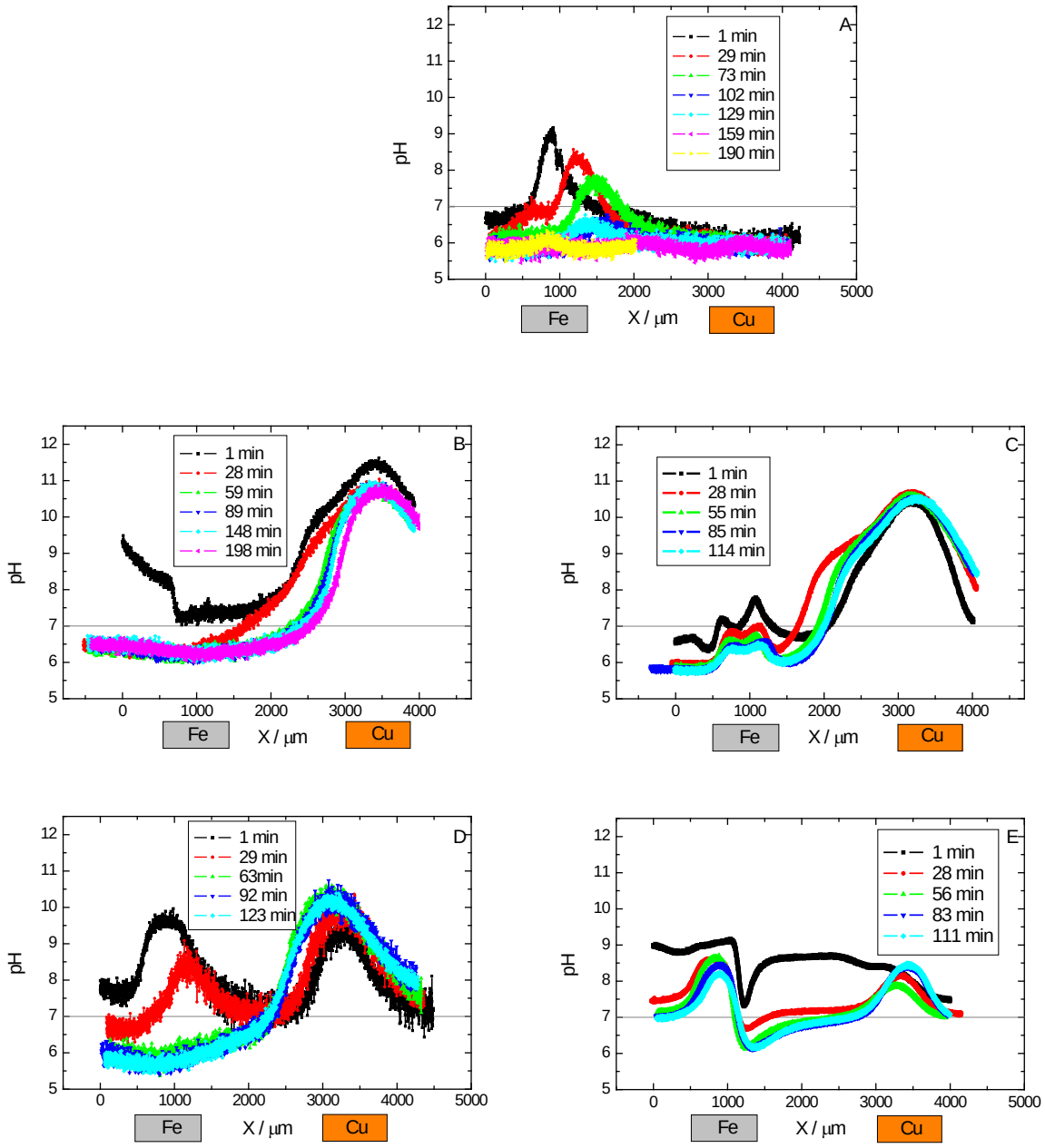

Figure 5

Local pH distribution lines generated by SECM with an antimony tip passing over the center of iron-copper samples subjected to different pretreatments with BTAH. The measurements were performed in 10 mM NaCl. Electric and surface conditions of the samples are the same described in the legend of Figure 3. Scan lines were initiated when the samples were immersed in the test solution for the times given in the plots. Tip-substrate distance: 25 µm.

Figure 6

Optical micrographs of the Fe-Cu sample immersed in 10 mM NaCl: (A) Just after immersion in the electrolyte; (B) after 3 hour exposure. No electric contact existed between the two metals.

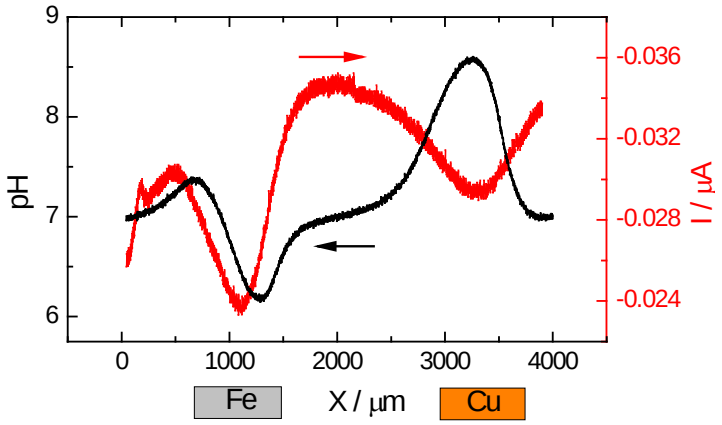

Figure 7

Line scans generated by SECM with an antimony tip passing over the centres of an iron-copper galvanic pair immersed in 10 mM NaCl for 3 hours. SECM operations: (black) potentiometric for pH monitoring, and (red) amperometric for the electroreduction of soluble oxygen (E_{tip} = -0.65 V vs. Ag/AgCl/3M KCl). Tip-substrate distance: 25 µm.

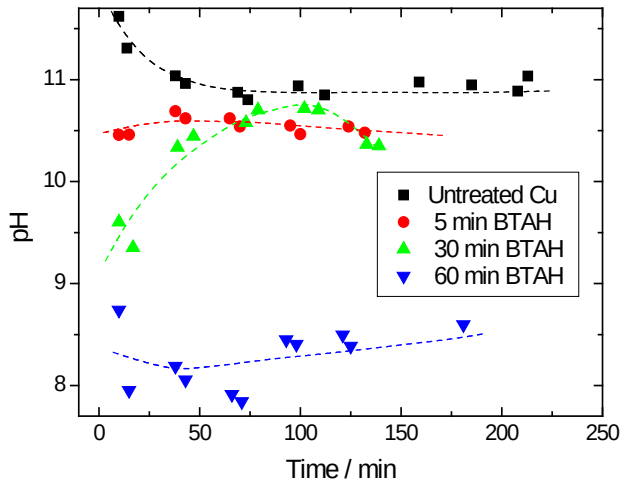

Figure 8

Time evolution of the maximum pH values measured over the copper sample taken from the curves displayed in Figure 5 B-E. They are a measure of the cathodic activity occurring on copper galvanically-coupled to iron during immersion in 10 mM NaCl.

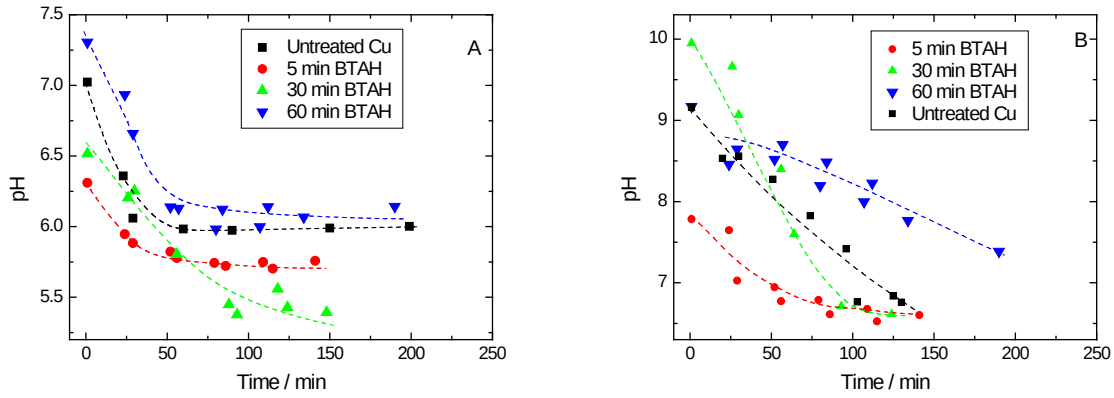

Figure 9

Time evolution of the (A) minimum and (B) maximum pH values measured over the iron sample taken from the curves displayed in Figure 5 B-E. They are a measure of the (A) anodic and (B) cathodic activity occurring on iron galvanically-coupled to copper during immersion in 10 mM NaCl.